What the Murchison Meteorite Reveals about Magnetic Fields in the Solar System's Protoplanetary Disk Formation

Gabriel Maxemin

Advisor: Roger Fu

ASTRON 98: Junior Thesis

Harvard College

December 2022

Abstract

The early history of our solar system involved protoplanetary disk formation, where mass accreted inwards towards the developing star. Observations of protoplanetary disks show that in order to sustain inward mass transfer, angular momentum must have been transferred outward. However, the mechanism that drives this outward angular momentum transfer is not well understood. Previous research suggests that magnetic fields could have played a role in this transfer. In addition, "dusty olivine," which can be found in chondrites, is thought to be a reliable recorder of magnetism in the early solar system. We analyze a sample of the Murchison meteorite, a carbonaceous chondrite, and uncover the magnetic properties of the meteorite to gain insight on the magnetic fields present during active disk accretion. We employ a quantum diamond microscope (QDM), capable of seeing magnetism at a fine scale of ~1 μm, to measure the magnetism of dusty olivine-bearing chondrules (DOCs) within the Murchison meteorite. In order to identify the DOCs, we cut 200-300 μm slices of the meteorite. We isolated four DOCs from the surrounding matrix of the meteorite and ran three of the four through a sequence of alternating-field (AF) demagnetization. One DOC shows clear components of magnetization, indicating the presence of a magnetic field during disk accretion. We plan to obtain a magnetic field estimate for this DOC by applying an anhysteretic remanence (ARM). The remaining two DOCs have not finished their AF demagnetization. We hope to continue analyzing DOCs from more slices and completing an AF demagnetization for these DOCs. Additionally, by comparing resulting magnetic properties with bulk meteorite magnetic field estimates, we can infer whether the chondrules formed locally or in a different environment.

Introduction

The early history of the solar system involved protoplanetary disk formation. The precursor to the protoplanetary disk was a cloud of molecular gas that began to collapse under its own weight. The cloud had a net angular momentum, and as the collapse continued, the cloud rotated faster to conserve angular momentum. Continued collapse allowed for the formation of a central mass, the Sun, and the remaining mass orbited this central mass. The remaining mass that was rotating flattened out, developing into the disk (Hartmann 2009). Observations of protoplanetary disks show that there must have been sustained, efficient inward mass transfer, necessitating outward angular momentum transfer. This is because in order for mass to fall inwards towards the developing star, the mass must lose angular momentum, so angular momentum must be transferred outward.

The mechanism driving the accretion of the protoplanetary disk along with angular momentum transport is not well understood and it is suspected that magnetic fields played a major role in this process. Among the proposed physical mechanisms of angular momentum transfer are magnetorotational instability (MRI) and magnetized disk winds. According to Weiss, Bai, and Fu (2021), we can think of MRI by considering two fluid parcels at different heights on an edge-on view of the protoplanetary disk. If one parcel is displaced more radially inwards, it will orbit faster than the other. A curved field then arises from the displacement, and a spring-like magnetic tension tries to bring the parcels back to their original positions. This tension increases as the parcels separate. Torque from the spring decreases the angular momentum for the inner parcel, while increasing it for the outer one. They also describe the magnetized disk wind mechanism, where the molecular cloud that the disk originates from is magnetized and passes on bent magnetic fields as it collapses, so the disk is threaded by a net

poloidal field. Keplerian shear of the radial component of the poloidal field at the disk surface gives rise to a toroidal field. Magnetic pressure builds up from the strengthening of the toroidal field, launching a wind. As the toroidal field strengthens, the poloidal fields are pinched together against the direction of rotation, and the torque associated with this pinching opposes the direction of rotation, so angular momentum is extracted from the disk (Weiss, Bai, and Fu 2021).

In order to explore the angular momentum transfer, we can analyze the Murchison meteorite. The Murchison meteorite is a carbonaceous chondrite with chondrules that can be examined to reveal the early history of the solar system. The meteorite dates back to approximately 2-3 million years after the formation of the protoplanetary disk (Fujiya et al., 2012). Murchison is therefore a useful meteorite to study for understanding magnetic fields during active disk accretion. Chondrules in the meteorite contain “dusty olivine” grains which are magnesium-rich olivine grains with iron inclusions that are reliable records of early solar system magnetism (Uehara and Nakamura, 2006; Lappe et al., 2013). Studying this chondrite will give insights into the magnetic field environment in the protoplanetary disk and test the mechanism of angular momentum transport. Fu et al. (2014) explain how during rock cooling, the chondrules acquired a thermoremanent magnetization (TRM) if they were in the presence of a stable magnetic field. Then, if we are able to know the magnetization of the chondrules as well as how easily they acquire a TRM, we can understand the magnetic field present during cooling.

In measuring the chondrite samples, we are looking at the Natural Remanent Magnetization (NRM) of the chondrite. NRM is the remanent magnetization of a rock without any lab treatment (Butler 1992). Present in rocks are two components of NRM that a rock acquires during its history: primary NRM and secondary NRM. A rock acquires primary NRM during rock formation, whereas it acquires secondary NRM subsequent to rock formation (Butler

1992). For the Murchison meteorite, we are interested in the magnetic fields present during chondrite's formation, making primary NRM the relevant component to investigate.

Methodology

A brief overview of the methodology can be seen in Figure 1. We performed all of the described steps in a magnetically clean environment so as to minimize any magnetic contamination in the samples and instruments. We used a wire saw to cut thin slices of the meteorite, then identified and extracted DOCs from these slices. Then, we used the quantum diamond microscope (QDM) to make magnetic field maps of the DOCs. We applied an alternating field (AF) demagnetization to the sample and then measured the magnetization on the QDM, repeating this step and increasing the field applied by 25 G each time. This allowed us to measure the NRM of the sample. After the AF demagnetization sequence used to measure the NRM, we applied an anhysteretic remanence (ARM) and put the sample through the same AF demagnetization sequence as with the NRM, measuring the magnetization on the QDM after each step in the sequence. This then gave us two sets of data, one measuring the NRM and one measuring the magnetization after ARM.

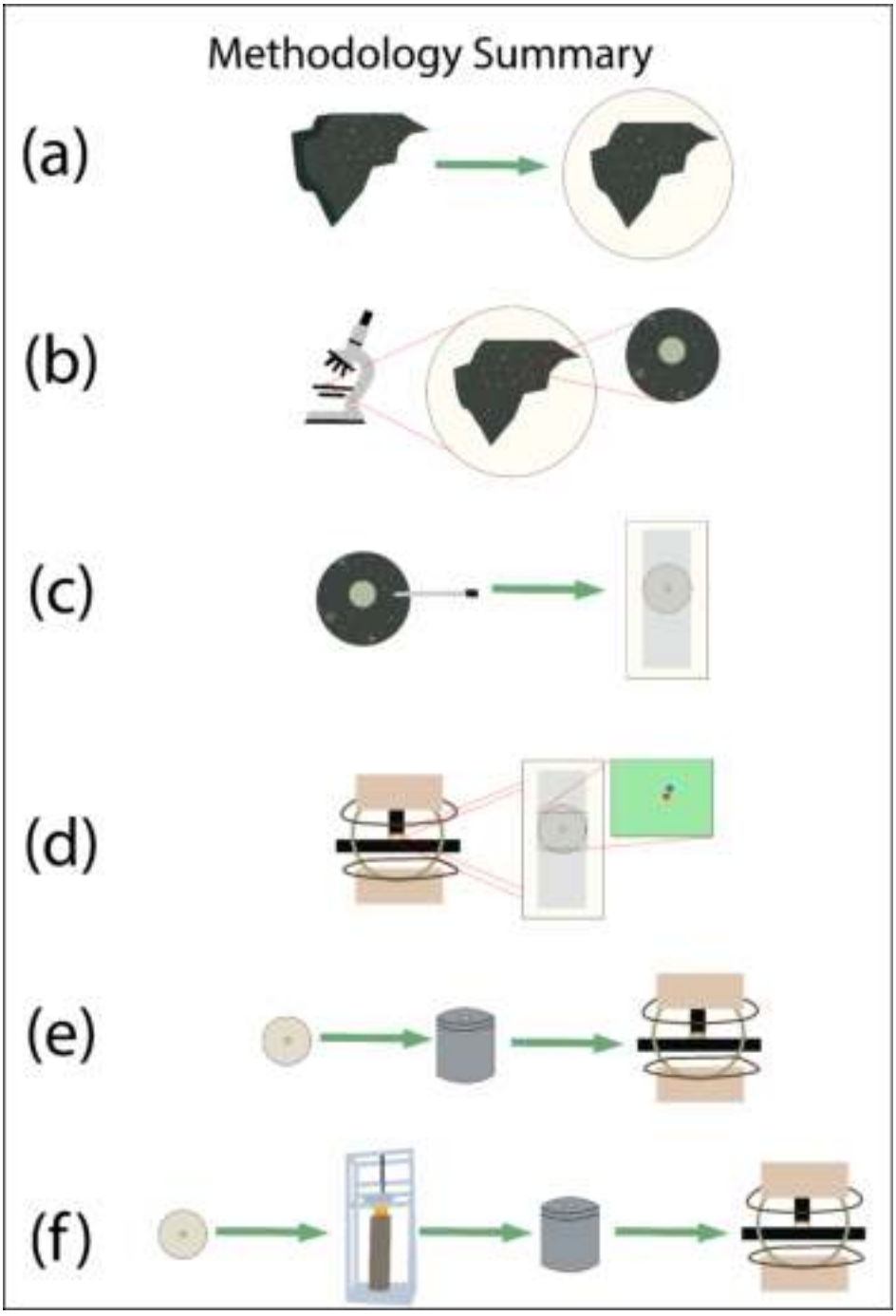

Figure 1. Summary of the methodology. (a) We made 200-300 μm slices of the meteorite. (b) Using a compound microscope, we scanned the thin slices and identified DOCs. (c) We drilled around the DOC to isolate it and placed the DOC on a glass slide. (d) The QDM produced a magnetic field map of the DOC. (e) We placed the DOC on a demagnetizer to apply an AF demagnetization and then obtained a magnetic field map on the QDM. This step was repeated, increasing the demagnetization after each step. (f) We put the DOC on a 2G magnetometer to apply an ARM and then put the DOC through the same AF demagnetization sequence as in step e.

Isolating DOCs from Murchison Meteorite

The Paleomagnetics Lab at Harvard University acquired a sample of the Murchison meteorite, pictured in Figure 2. In order to identify DOCs, we used a wire saw to cut 200-300 μm slices of the meteorite. The DOCs are generally around 0.5 mm in radius. A sample slice is pictured in Figure 2. A piece of the meteorite was glued onto a glass slide and the wire saw cut out most of the meteorite so as to leave only the thin slice on the slide. After slicing, the samples were given a light polish. We used a compound microscope to look for DOCs on both sides of the slide: the glass side and the exposed sample side. Figure 3 shows DOC 1.10 under three levels of magnification on the compound microscope. We identified DOCs by looking for bright silver inclusions within chondrules under 20x magnification. Once we identified these chondrules, we confirmed that they contained dusty olivine by checking that there was a striated pattern, as is visible in Figure 3 under 50x magnification. Once the DOCs were identified, they were extracted using a drill. Isolating the DOCs allowed us to minimize any signal sourced from the matrix of the chondrite or from other chondrules.

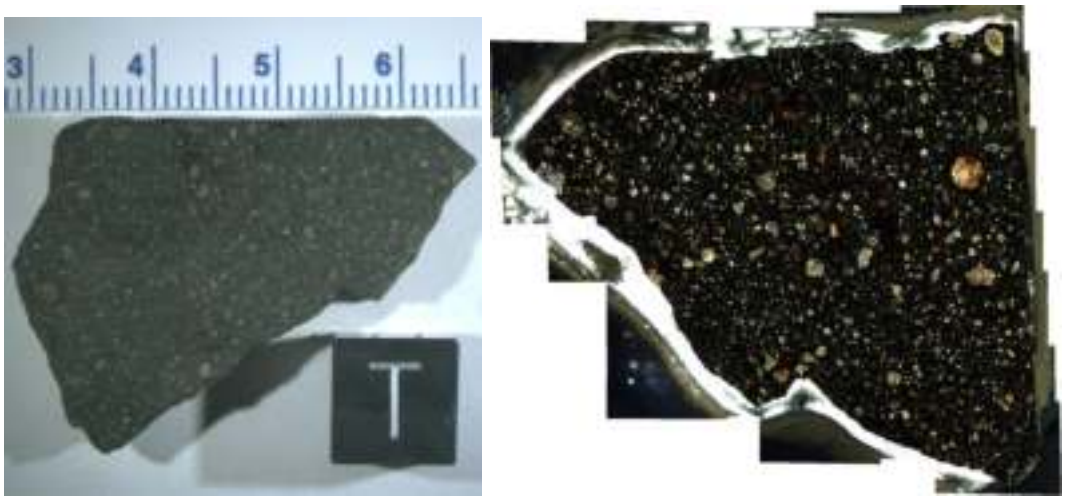

Figure 2. (left) Full sample of the Murchison meteorite retrieved by the Paleomagnetics Lab at Harvard University. (right) 200-300 μm thin slice of the Murchison meteorite.

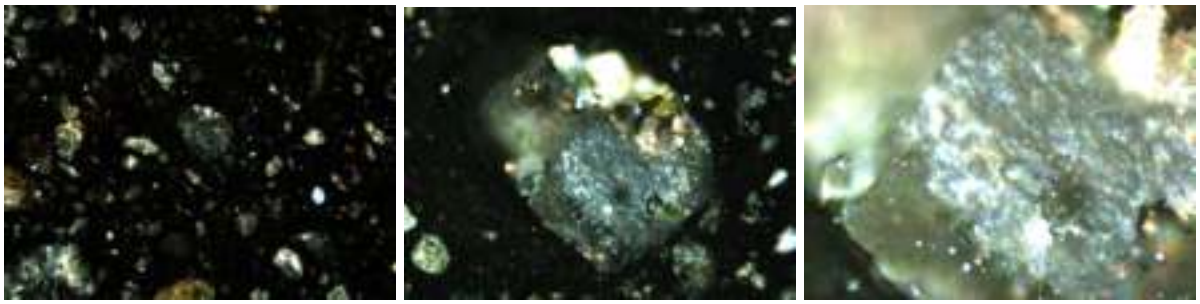

Figure 3. DOC 1.10 under the compound microscope. (left) 5x magnification. (middle) 20x magnification. (right) 50x magnification.

Quantum Diamond Microscope

Precise magnetic measurements of the meteorite samples were possible because of the Quantum Diamond Microscope (QDM). The QDM allows for the visualization of magnetism at a fine scale of ~1 μm. We used the QDM to obtain a magnetic field map of a DOC. Then, we fit this map to a dipolar source model. This allowed us to quantify the net magnetization of the chondrule. In order to obtain the dipolar source model, some data processing is involved. To ensure that the signal we measure is not an external artifact, such as a magnetic source coming from the diamond on the QDM, we ran a blank sample on the QDM and subtracted this data from the DOC data. The result is then a blank-subtracted magnetic dipole map from which we select the region containing the dipole to find a dipole model that best fits this dipole.

Alternating-Field Demagnetization

In order to remove secondary NRM from the DOCs, we employed AF demagnetization. AF demagnetization involves exposing the sample to an alternating magnetic field that is sinusoidal and decreases linearly in magnitude over time, erasing the net effect of all grains in the sample that are magnetized below the applied alternating magnetic field; this method is effective at

removing secondary NRM since primary NRM are generally more resistant to heating (Butler 1992).

The alternating field was applied on all three axes to ensure that the demagnetization was random. For each DOC, we began by measuring the DOC on the QDM without any demagnetization. Then, we applied an AF demagnetization of 50 G and measured the DOC on the QDM, comparing the results from before and after demagnetization. Each DOC then underwent an AF demagnetization sequence; we increased the magnitude of AF demagnetization by 25 G from the previous demagnetization, then used the QDM to measure the DOC, and then repeated this sequence until the magnetization of the DOC changed randomly. A random change in magnetization implies that all remanence-carrying grains have been reset. This is because, if a sample is already fully demagnetized, applying more AF demagnetization will merely re-randomize the grains.

The AF demagnetization sequence was terminated whenever the magnetization changed randomly upon repeat AF demagnetization of the same field magnitude. For example, random changes in magnetization after applying an AF demagnetization of 700 G five different times indicates that the AF demagnetization sequence should end. Based on the QDM results, this meant that the morphology of the magnetic dipoles changed drastically or that the magnetic moment magnitude changed by a factor greater than 2. What constitutes a drastic change in morphology is if the directionality of the morphology changes by more than 90 degrees or if the source no longer resembles a dipole.

Anhysteretic Remanence

After we put a DOC through an entire AF demagnetization sequence, we can have a sense of the NRM of the DOC. However, this information alone cannot tell us the temperature that the DOC was heated during rock formation and hence cannot inform us on the strength of the magnetic field that the DOC was in. This is because we don't know how easily a DOC acquires a magnetic field. For this reason, we simulate the acquisition of TRM using ARM. TRM is the remanence a rock acquires upon being subjected to a magnetic field that cools the rock from a temperature above its Curie temperature to a lower temperature (Schön 2011). We used a 2G magnetometer to subject the DOC to ARM. For DOC 1.06, we applied an ARM with an AC field of 3000 G and a bias field of 1.99 G. After applying the ARM, we put the DOC through the same AF demagnetization sequence that it was subjected to when measuring its NRM.

Protoplanetary Disk Magnetic Field Intensity

For each DOC, we are left with two sets of data, one from the NRM AF demagnetization sequence and another from the ARM AF demagnetization sequence. From this, we can calculate the magnetic field intensity at the time of the DOC formation, giving us an idea of the magnetic field present during protoplanetary disk formation. We calculate the magnetic field intensity $B_{paleointensity}$ with

$$B_{paleointensity} = \frac{\triangle N}{\triangle A} \cdot B_{bias} \cdot \mathrm{c}$$

where $\triangle$N is the vector change in magnetization of the DOC at each step of the NRM AF demagnetization sequence, $\triangle$A is the vector change in magnetization of the DOC at each step of the ARM AF demagnetization sequence, B_{bias} is the bias field applied for the ARM, and c is a

correction factor. The correction factor c comes about because the paleointensity of the DOC's NRM is lower than the magnetic field used in the lab. This is because the DOC's NRM was likely not acquired by an alternating field but instead through thermal magnetization. Since it is easier to remagnetize a rock of higher temperature, the actual NRM paleointensity is lower by this correction factor.

Results

We extracted four DOCs from the Murchison meteorite sample, three from one slice and one from another. One DOC extracted from the first thin slice, named DOC 1.10, was subject to an NRM AF demagnetization sequence up to 1100 G but has yet to receive an ARM. DOC 1.06 was subject to both an NRM and ARM AF demagnetization sequence up to 350 G. DOC 1.09 is at 250 G in its NRM AF demagnetization sequence but still needs to progress through more of this sequence. DOC 2.01 has not begun its NRM AF demagnetization sequence. Some examples of QDM outputs from the NRM AF demagnetization sequence are laid out in Figure 4. Inspecting Figure 4 qualitatively, the progression from 100 G to 225 G did not drastically change the morphology of the dipole. However, the morphology does appear to change at greater AF demagnetization. For example, at 900 G, the dipole begins to take on a different shape than the one seen at 200 G, and by 1100 G the dipole appears to have changed much more drastically. The sample after a 100 G AF demagnetization had a magnetic moment of 1.35705e-12 A*m^2, the 225G one had a moment of 1.36409e-12 A*m^2, the 900G had a moment of 4.52989e-13, and the 1100 G one had a moment of 3.36417e-13 A*m^2.

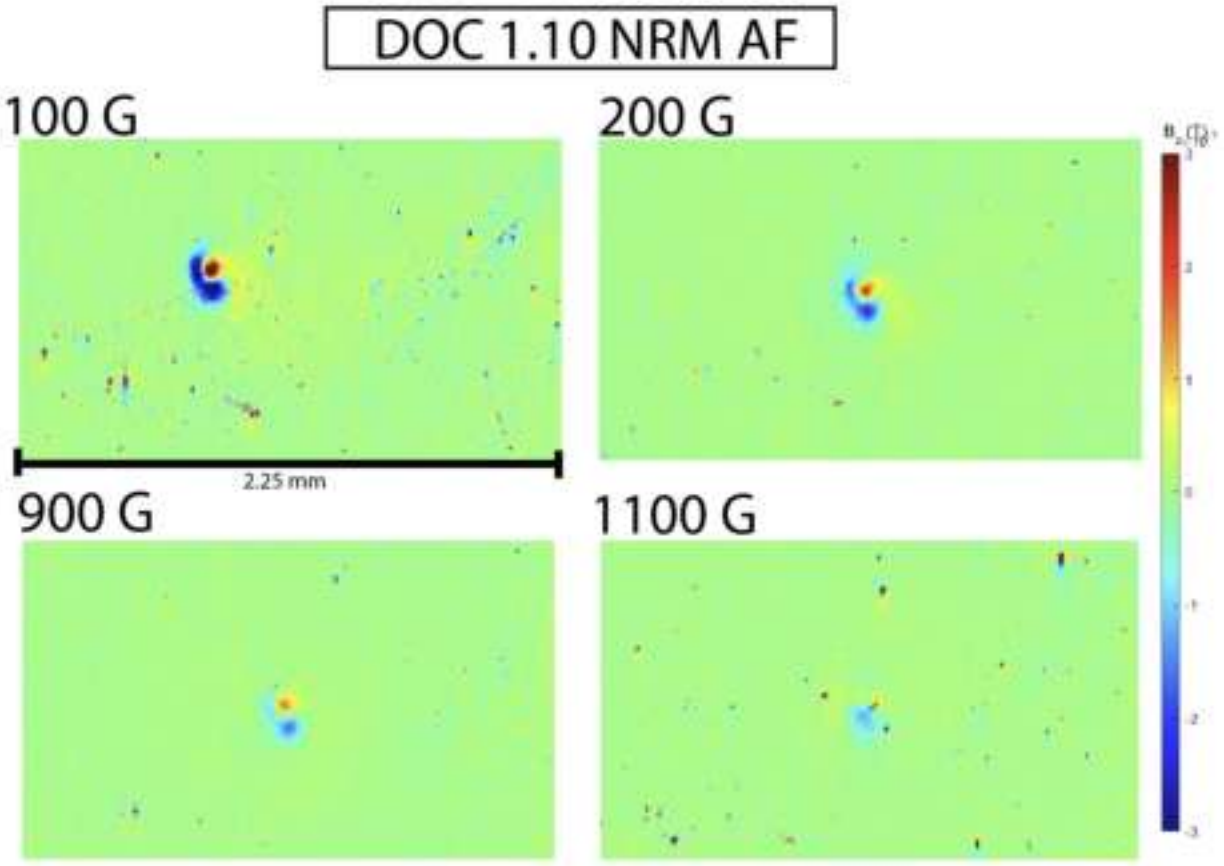

Figure 4. Dipole visualization of DOC 1.10 obtained from the QDM after different NRM AF demagnetization steps. Top left shows AF demagnetization of 100 G, top right shows 225 G, bottom left shows 900 G, and bottom right shows 1100 G.

Figure 5 shows the vector component diagram for DOC 1.10. A vector component diagram is useful in informing whether secondary NRM has been removed and whether we have a clear component of magnetization from the sample. As NRM is removed, a vector component diagram shows decreasing intensity as the distance of a data point to the origin decreases (Butler 1992). Once the secondary NRM component is removed, the sequence of vectors pointing from the origin to the data points only has the primary NRM component, meaning there is only a decrease in magnitude and not of direction, visualized as a linear trend towards the origin (Butler 1992). On the right diagram of Figure 2, we can see an approximate linear trend towards the

origin. This can be seen more easily by paying attention to the points of inclination. The leftmost point indicates the starting point in the AF demagnetization sequence. As the graph progresses, we remove secondary NRM, until we reach the sixth point, where we begin to see a linear trend towards the origin. From this, we learn the magnetization of DOC 1.10. However, we still need to apply an ARM to obtain an estimate of the magnetic field in the protoplanetary disk during this DOC's formation.

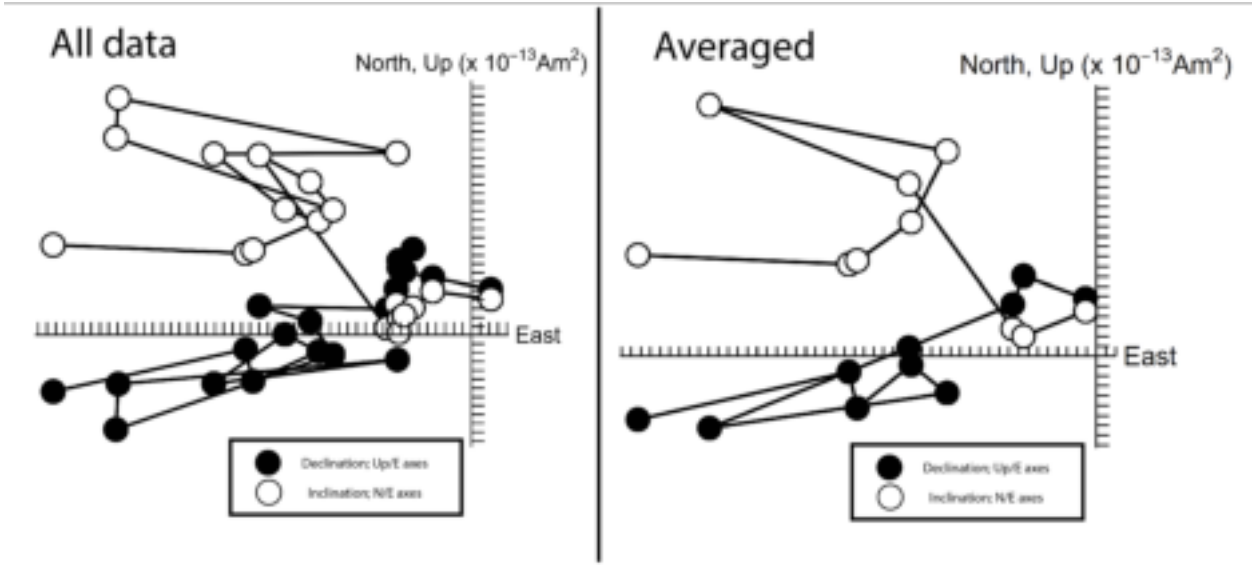

Figure 5. Vector component diagram of DOC 1.10 with data points from 50 AF demagnetization to 1100 G AF demagnetization. (left) Shows all data points. (right) Shows averaged data points. We selected certain groups of steps to average in order to create a cleaner graph for visualization

Figure 6 and Figure 7 both display AF demagnetization sequences for DOC 1.06. Figure 6 shows the NRM sequence and Figure 7 shows the ARM sequence. In contrast to DOC 1.10, DOC 1.06 became demagnetized at a much lower NRM AF demagnetization than DOC 1.10. Once the DOC reached 275 G, we began to see large changes in the dipole morphology.

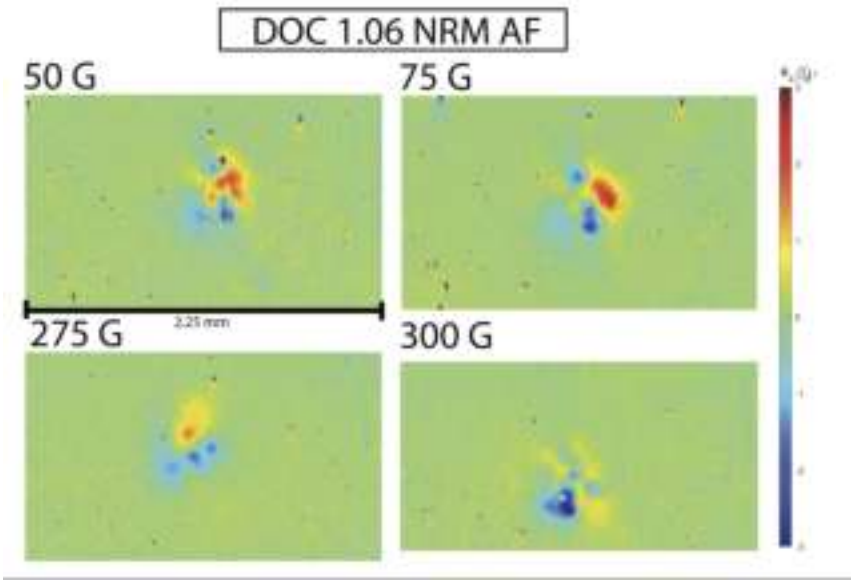

Figure 6. Dipole visualization of DOC 1.06 obtained from the QDM after different NRM AF demagnetization steps. Top left shows AF demagnetization of 50 G, top right shows 75 G, bottom left shows 275 G, and bottom right shows 300 G.

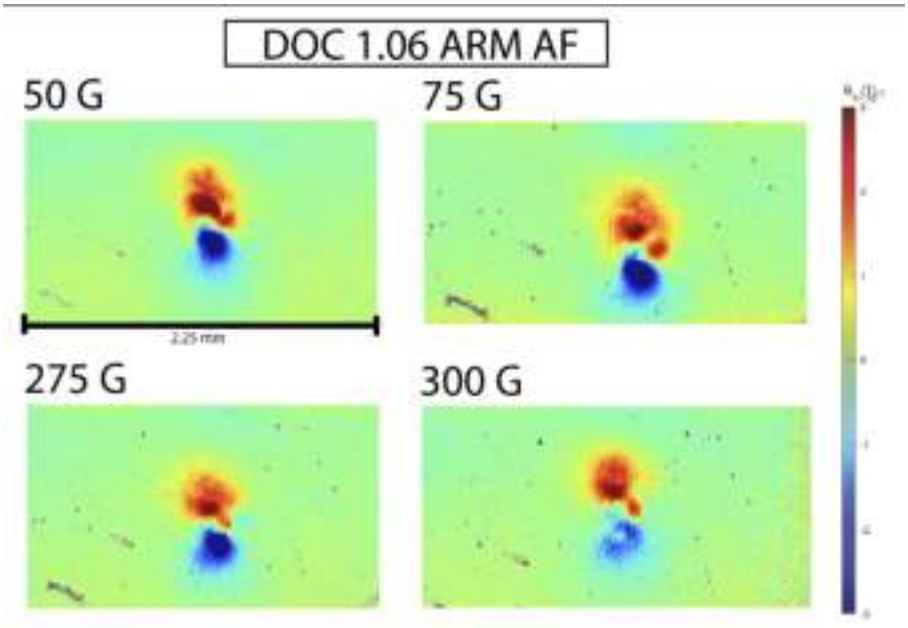

Figure 7. Dipole visualization of DOC 1.06 obtained from the QDM after different ARM AF demagnetization steps. Top left shows AF demagnetization of 50 G, top right shows 75 G, bottom left shows 275 G, and bottom right shows 300 G.

Table 1 and Table 2 show the magnetic moment measurements for DOC 1.06 after different steps of AF demagnetization. Table 1 shows the NRM sequence and Table 2 shows the ARM sequence. The dipolarity measurement reports how closely the magnetic field mapping of the DOC resembles a dipole. A vector component diagram of this data would establish whether we have isolated primary NRM and have a clear component of magnetization. We would then be able to obtain a paleointensity measurement since we have both NRM and ARM data.

AF	Moment (A*m^2)	Inclination (°)	Declination (°)	Dipolarity
50G	3.01E-12	-1.62113	41.5411	0.862246
75G	3.47E-12	-2.7847	54.6596	0.874541
100G	8.06E-12	-16.3052	72.0118	0.880006
150G	4.94E-12	-13.0623	58.7997	0.891644
175G	3.47E-12	2.16361	54.7137	0.848566
200G	1.78E-12	4.20804	83.7062	0.795322
200G_rep	3.10E-12	13.4962	64.0326	0.812509
225G	2.14E-12	17.406	63.9131	0.764093
250G	2.58E-12	21.6209	59.2303	0.723226
275G	4.47E-12	9.32278	12.8669	0.575608
300G	2.93E-12	44.0494	87.9247	0.715121
300G_rep	4.32E-12	30.4274	357.899	0.471492
325G	2.24E-12	14.6309	54.4791	0.73819
350G	2.46E-12	20.9634	74.7543	0.5936
350G_rep	3.14E-12	38.8922	95.6684	0.4575

Table 1: DOC 1.06 NRM AF demagnetization sequence

AF	Moment (A*m^2)	Inclination (°)	Declination (°)	Dipolarity
50G	8.81E-12	-6.9376	355.025	0.713136
75G	7.45E-12	0.647085	359.777	0.762946
100G	1.53E-11	5.08625	358.16	0.802735
150G	8.92E-12	-6.57514	355.013	0.717522
175G	9.94E-12	-6.5587	347.117	0.749944
200G	9.70E-12	7.00919	330.832	0.715595
225G	8.64E-12	8.44785	334.039	0.698095
250G	7.01E-12	-3.62881	342.284	0.7238
275G	8.72E-12	7.28573	346.621	0.725919
300G	7.31E-12	-21.3058	345.491	0.701135
325G	7.04E-12	-13.6221	357.938	0.722932
350G	9.01E-12	-19.6919	7.09438	0.737728

Table 2: DOC 1.06 ARM AF demagnetization sequence

Discussion

The linear trend towards the origin in the right diagram of Figure 5 indicates that secondary NRM has been removed for DOC 1.10 and that there is a clear component of magnetization present in the sample. This is a significant finding since this data comes from using the high-resolution QDM, and we can be more confident that this magnetization comes from the DOC itself since we measured it in isolation of the surrounding matrix.

Although we cannot yet draw conclusions from the other DOCs, we have advanced significantly in learning about the DOCs through their AF demagnetization sequence. For example, DOC 1.10 and DOC 1.06 differed greatly in the field strength that they became demagnetized at when trying to measure NRM. Different factors could explain this difference, such as simply a difference in grain size. However it will be exciting to learn what the paleointensity results are for each of these chondrules.

We plan on putting DOC 1.09 and DOC 2.01 through their NRM AF demagnetization sequence. Then, we hope to put these DOCs along with DOC 1.10 through an ARM AF demagnetization sequence. From this, we can get an idea of the background protoplanetary disk field present when the DOCs cooled. We also plan on isolating more DOCs and putting them through the same sequence of steps in order to have a more concrete result. Then, comparing our results with magnetic field estimates of the bulk Murchison meteorite will give us insight into whether the chondrules formed locally within the meteorite or externally.

References

Butler, Robert. (1992). *Paleomagnetism: Magnetic Domains to Geologic Terranes*. Blackwell Science Inc..

Fu, R. R., Weiss, B. P., Lima, E. A., Harrison, R. J., Bai, X.-N., Desch, S. J., Ebel, D. S., Suavet, C., Wang, H., Glenn, D., Le Sage, D., Kasama, T., Walsworth, R. L., & Kuan, A. T. (2014). Solar nebula magnetic fields recorded in the SEMARKONA meteorite. *Science*, 346(6213), 1089–1092. https://doi.org/10.1126/science.1258022

Fujiya, W., Sugiura, N., Sano, Y., & Hiyagon, H. (2013). Mn–cr ages of dolomites in CI chondrites and the tagish lake ungrouped carbonaceous chondrite. *Earth and Planetary Science Letters*, *362*, 130–142. https://doi.org/10.1016/j.epsl.2012.11.057

Hartmann, L. *Accretion Processes in Star Formation*: Second Edition; Cambridge University Press, Cambridge, 2009.

Lappe, S. C. L., Feinberg, J. M., Muxworthy, A., & Harrison, R. J. (2013). Comparison and calibration of nonheating paleointensity methods: A case study using Dusty Olivine. *Geochemistry, Geophysics, Geosystems*, *14*(7), 2143–2158. https://doi.org/10.1002/ggge.20141

Schön, S. J. (2011). Magnetic properties. *Handbook of Petroleum Exploration and Production*, 8, 373–391. https://doi.org/10.1016/s1567-8032(11)08010-4

Uehara, M., & Nakamura, N. (2006). Experimental constraints on magnetic stability of chondrules and the paleomagnetic significance of Dusty Olivines. *Earth and Planetary Science Letters*, *250*(1-2), 292–305. https://doi.org/10.1016/j.epsl.2006.07.042

Weiss, B. P., Bai, X.-N., & Fu, R. R. (2021). History of the solar nebula from Meteorite Paleomagnetism. *Science Advances*, *7*(1). https://doi.org/10.1126/sciadv.aba5967

Acknowledgements

I would like to thank my advisor, Roger Fu, for guiding me through this project and Sarah Steele for helping me with plotting and understanding concepts. I would also like to thank David Wilner for his feedback on my Junior Thesis. In addition, I thank Professor Ramesh Narayan for supporting our ASTRON 98 class throughout our projects.